Comparison of 1D and 2D liquefaction assessment methods considering soil spatial variability

Gonzalez Acosta, J.L.; van den Eijnden, A.P.; Hicks, M.A.

Comparison of 1D and 2D liquefaction assessment methods considering soil spatial variability

J.L. González Acosta, A.P. van den Eijnden, and M.A. Hicks

Geo-Engineering Section, Faculty of Civil Engineering and Geosciences,
Delft University of Technology, The Netherlands.
E-mail: J.L.GonzalezAcosta-1@tudelft.nl, A.P.vandenEijnden@tudelft.nl, M.A.Hicks@tudelft.nl

Abstract: 1D soil column techniques are widely used to evaluate the potential of liquefaction in a system of soil layers. This approach generally leads to large inaccuracies since (1) soil layers are hardly homogeneous and perfectly horizontal and (2) horizontal effects are neglected. To demonstrate the limitation of 1D strategies and the need for 2D simulations, a series of benchmark problems are proposed and studied considering a fully coupled RFEM framework with small strain effects to account for cyclic behavior. First, a 1D simulation of a homogeneous material is tested against similar 1D problems including the spatial variation of soil properties (in this case void ratio). Then, a 2D domain is analyzed using the void ratio distribution obtained from combining the 1D columns. This investigation demonstrates that, by combining the effects of the horizontal direction and the spatial distribution of the soil properties, liquefaction triggering, spatial spreading and propagation extent may change significantly.

Keywords: Coupled behavior; earthquakes; hypoplasticity; liquefaction; random fields.

1 Introduction

Soil liquefaction is a phenomenon which is not fully understood. It is established that liquefaction occurs when the excess pore water pressure exceeds the initial effective stresses at a certain location, leading to the complete loss of soil bearing capacity and the collapse of its structure. However, the understanding of soil liquefaction triggering and spreading when the spatial distribution of soil properties is not ideal (i.e. homogeneous and horizontally layered) remains unclear. A main reason influencing this persisting lack of understanding is that most of the studies are performed using 1D models of ideal materials, thus ignoring realistic soil spatial variability and omitting horizontal effects. Some studies of soil liquefaction have been performed incorporating soil spatial variability. Nevertheless, such studies often use fields of soil spatial variability assigned to 1D columns, therefore disregarding the horizontal interaction between the columns (Fenton and VanMarcke 1998), or focus only on the analysis of specific case histories (Popescu et al. 2005). This paper provides some insights into soil liquefaction in a stochastic context, including consideration of horizontal effects. First, the concepts of the random finite element method (RFEM) and random field theory are introduced. Then, a 1D benchmark is presented to be used as a reference solution for subsequent simulations. Afterwards, a 2D domain is simulated including soil property variability, followed by the simulation of multiple 1D columns constructed with the same soil properties as the 2D domain. The combined results of the 1D columns are compared against the full 2D simulation, therefore providing a reliable contrast of 1D simulations against 2D. Liquefaction is assessed through (i) a standard liquefaction index q_i, and (ii) the liquefied area (A_L). Finally, cyclic and small strain soil behaviours are achieved through hypoplasticity, whereas the coupled hydro-mechanical behavior is considered through a *u-p* formulation.

2 Random finite element method theoretical background

The random finite element method (RFEM) is a technique that combines standard finite element (FE) analysis with random field theory to come towards more realistic predictions of soil failure mechanisms (Griffiths and Fenton 2004). RFEM has been mostly used to study slope stability problems (e.g. Varkey et al. 2020), but it can be implemented to study most soil failure problems, including liquefaction (Hicks and Onisiphorou 2005). RFEM involves Monte Carlo simulations, where a number of simulations (realizations) are computed using different random fields of soil property values in order to find the distribution of possible solutions. Regarding the distribution of soil properties, conventional methods are used to construct random fields $\mathbf{X}(\bar{x})$ by first creating a standard normal random field $\mathbf{Z}(\bar{x})$ and then applying a transformation $\Psi(.)$ to obtain the desired random field of a variable X. Here, a lognormal random field $\mathbf{X}(\bar{x})$ is constructed as:

$$\mathbf{X}(\vec{x}) = \mathbf{\Psi}(\mathbf{Z}(\vec{x})) = \exp(\mu + \sigma\mathbf{Z}(\vec{x})), \quad \forall \vec{x} \in \Omega \qquad (1)$$

where μ and σ are the mean and standard deviation of $\ln(\mathbf{X})$, respectively. The transformation from standard normal fields provides flexibility in creating and manipulating the random fields. A number of strategies to create approximations of random fields have been developed, but those based on methods of covariance matrix decomposition are of particular interest because of their ability to describe the correlated random field (after discretization) as a linear function of a set of uncorrelated standard normal variables. Note that the spatial correlation between two points is achieved as:

$$\rho(\tau) = \exp(-2\tau); \quad \tau = \sqrt{\left(\frac{\Delta x_1}{\theta_1}\right)^2 + \left(\frac{\Delta x_2}{\theta_2}\right)^2} \qquad (2)$$

where $\rho(\bullet)$ is the correlation function, τ is the normalized distance with respect to the scales of fluctuation θ_i, and x_i are the coordinates of a Gauss point i. Since the finite element (RFEM) framework is implemented in this work, the total number of Gauss integration points are the maximum number of variables to discretize. The reader is directed to van den Eijnden and Hicks (2017) for more information regarding the construction of random fields.

3 Liquefaction assessment

To ensure an exhaustive study of liquefaction development considering soil spatial variability, first, a 1D solution of a homogeneous material is simulated and taken as the reference solution. Then, a domain of width $w = 20$ m and $h = 10$ m is created assuming material variability where the void ratio e is the main stochastic parameter (i.e. randomized parameter). This domain will be used to perform 1D and 2D liquefaction simulations, in which the 2D simulations contemplate the full domain and its material heterogeneity, whereas 1D simulations are performed by constructing 1D columns with material properties extracted from the 2D domain. The objective of comparing 2D simulations against their counterparts, split into 1D columns, is to analyse the effects of liquefaction (i) triggering and (ii) spreading (i.e. A_L in time) when horizontal effects are considered or neglected. This study resembles previous work in which a 2D domain was divided into 1D columns to study the effects of removing horizontal effects when computing settlements at the end of the consolidation process following on earthquake (Basu et al. 2019). In contrast, this study focuses on the timing of triggering and the growth of the liquefaction.

To account for the cyclic behaviour of the soil, the hypoplastic constitutive model with intergranular strain is adopted using parameters corresponding to a loose sand (Table 1). Regarding the construction of the random fields, a mean void ratio $e_\mu = 0.75$, standard deviation $e_\sigma = 0.03$, and scales of fluctuation $\theta_H = 4.0$ m and $\theta_V = 1.0$ m are used, where θ_H and θ_V are the horizontal and vertical scale of fluctuation, respectively. In this study, the original hypoplastic constitutive model with intergranular strain is used, and the full formulation and description of the required parameters can be found in Niemunis and Herle (1997) and Gudehus et al. (2008).

Table 1 Soil parameters

ϕ_c	p_t	h_s	n	e_{d0}	e_{c0}	e_{i0}	α	β	m_R	m_T	R	β_r	χ
(°)	(kPa)	(kPa)	-	-	-	-	-	-	-	-	-	-	-
32	1.0E^{-5}	1.5E^{-6}	0.27	0.4	0.8	1.1	0.18	1.1	5.0	2.0	1.0E^{-4}	0.5	6

The acceleration record used to simulate the earthquake corresponds to the Superstition Hills event (Figure 1). However, the simulated time was truncated at 12 s, since the seismic activity after 12 seconds proved to be inconsequential. Periodic boundary conditions are used to ensure realistic earthquake simulations (Cook et al. 1989) and a detailed description on the implementation of the coupled u-p hydro-mechanical formulation can be found in Zienkiewicz et al. (1999).
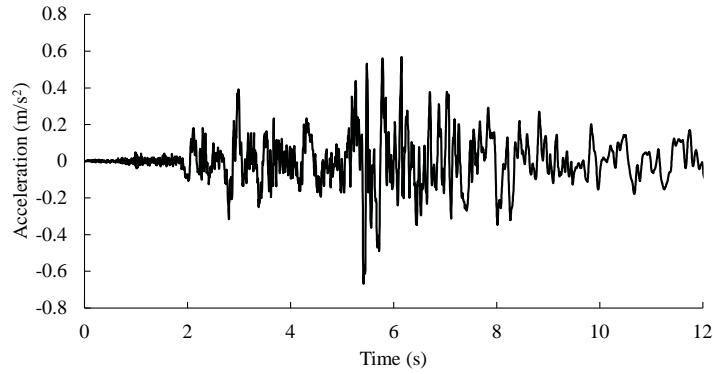
Figure 1. Recorded accelerogram during Superstition Hills event (North-South component)

4   Results

Liquefaction can be assessed through liquefaction indexes. In this paper, the index introduced by Seed (1979) is used and computed as $q_i = u_i / \sigma_{v,i}$, where q_i is the liquefaction index, u_i is the excess pore water pressure, and $\sigma_{v,i}$ is the initial vertical effective stress, with all variables measured at the element Gauss point i. Note that, for this work, nine node quadrilateral elements, of size 1 m × 1 m, with nine Gauss points per element are used. It is conventional to consider that liquefaction occurs when $q_i = 1.0$ (i.e. full stress taken by the water pressure), although it is also realistic to assume that liquefaction occurs an instant earlier, approximately when $q_i > 0.95$, which is the value considered herein (i.e. only values of q_i above 0.95 are considered for the measurement of A_L). The deterministic 1D column used as the reference solution is 1 m wide and 10 m high (i.e. 1 element horizontally and 10 elements vertically) and is simulated assuming a homogeneous soil using the mean void ratio $e_\mu = 0.75$. Figure 2 shows the results of the 1D deterministic simulation. It is observed in Figure 2a that, after the earthquake, liquefaction has been triggered close to the centre of the domain ($h \approx 5$ m). The liquefied zone is entirely horizontal with a thickness of 0.66 m (i.e. two rows of Gauss points).
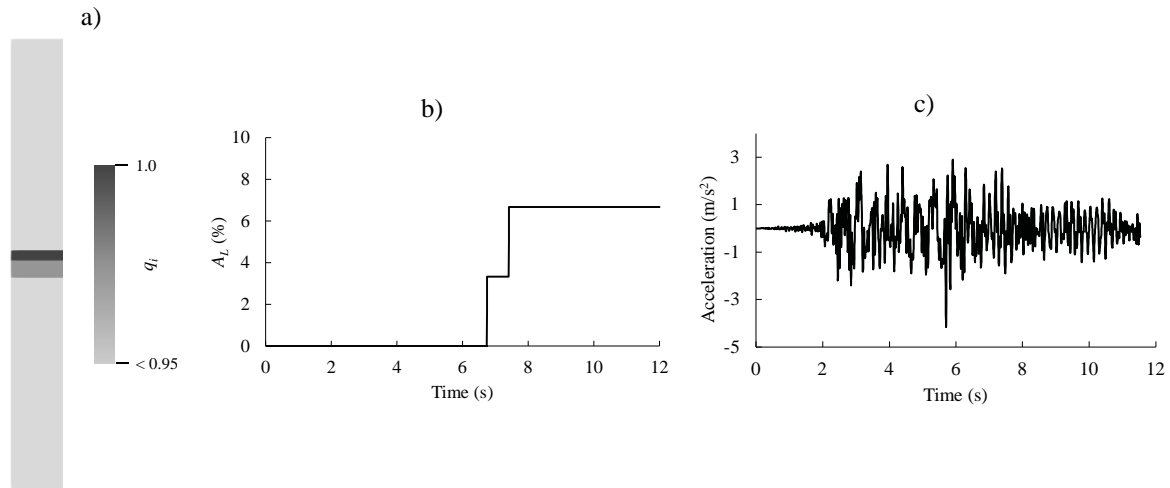

Figure 2. 1D column deterministic *D* solution: a) liquefaction index q_i after earthquake, b) liquefaction area A_L in time, and c) surface accelerations.

Figure 2b shows that, at $t = 6.52$ s, liquefaction is triggered, and the vertical line reaching $A_L = 3$ % indicates that a full row of Gauss points (i.e. three Gauss points) were triggered simultaneously. Note that this initial triggering occurs close to the maximum acceleration amplitude of Figure 2c. Later, at $t = 7.4$ s, a second row of Gauss points is triggered, below the previous one, as a consequence of the continuing earthquake. Figure 2 shows typical results of a standard liquefaction assessment. The most noticeable aspects of such 1D assessments, which are unlikely to occur in a real liquefaction problem, are that: (1) liquefaction develops in horizontal layers, and (2) the layers are fully (i.e. from the left to the right extremes) and instantaneously triggered at a particular time. Figure

3 shows the domain created to study horizontal effects. Figure 3a shows the 2D domain with a width (*w*) and depth (*h*) of 20 m and 10 m, respectively. The marks above Figure 3a (i.e. s^1,…, s^{20}) are the centre position of each column of elements and denotes where the properties of the soil were extracted vertically to construct the 1D columns of heterogeneous material. Figure 3b shows an example of a 1D column constructed using the properties extracted from s^1. Note that the properties used for the 1D columns are extracted from the 2D domain and extended horizontally, similar to as conducted in typical 1D liquefaction assessments.

Figure 4 shows the evolution of liquefaction with time for the domain shown in Figure 3a. Figure 4a shows the presence of some isolated pockets of soil fully liquefied. Nevertheless, the overall behaviour of the domain remains elastic. Figure 4b shows an extended liquefied zone that has not yet crossed the entire domain. Figure 4c shows that liquefaction has crossed the domain from side to side. It is important to notice in this figure that the thickness of the liquefied zone is not uniform as observed in typical 1D simulations (e.g. Figure 2a). Finally, Figure 4d shows the final step of the simulation, when the earthquake has almost ceased. A large liquefaction zone is observed and, despite the liquefaction growing rate having diminished, observation indicates that the liquefaction continues spreading slowly to the ground surface. This growth is caused mostly because of the remaining shear waves in the system and the lack of support beneath the elastic soil (i.e. liquefied soil not supporting the soil above).
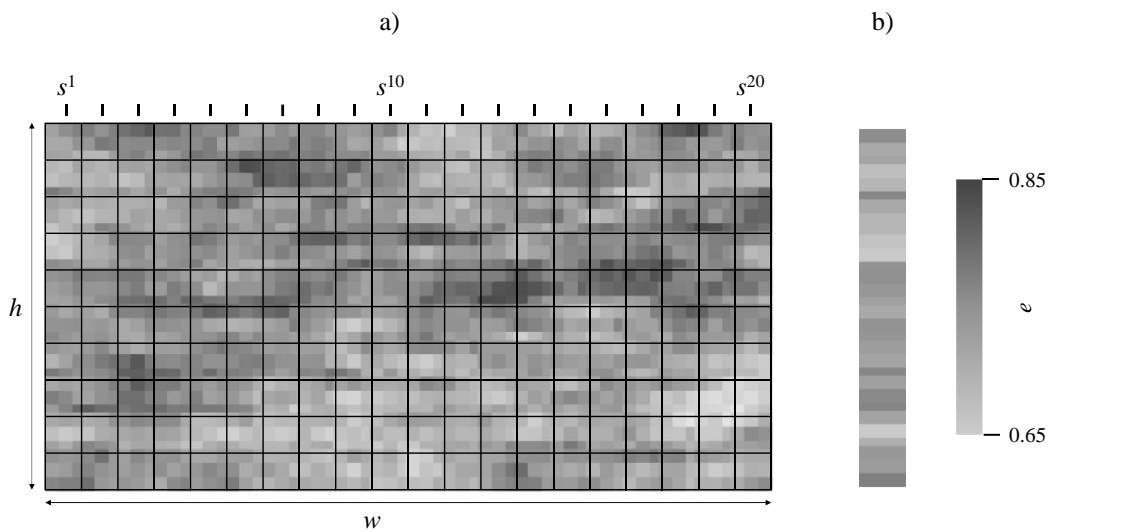

Figure 3. Typical void ratio *e* distribution over a) the 2D domain, and b) a 1D column.
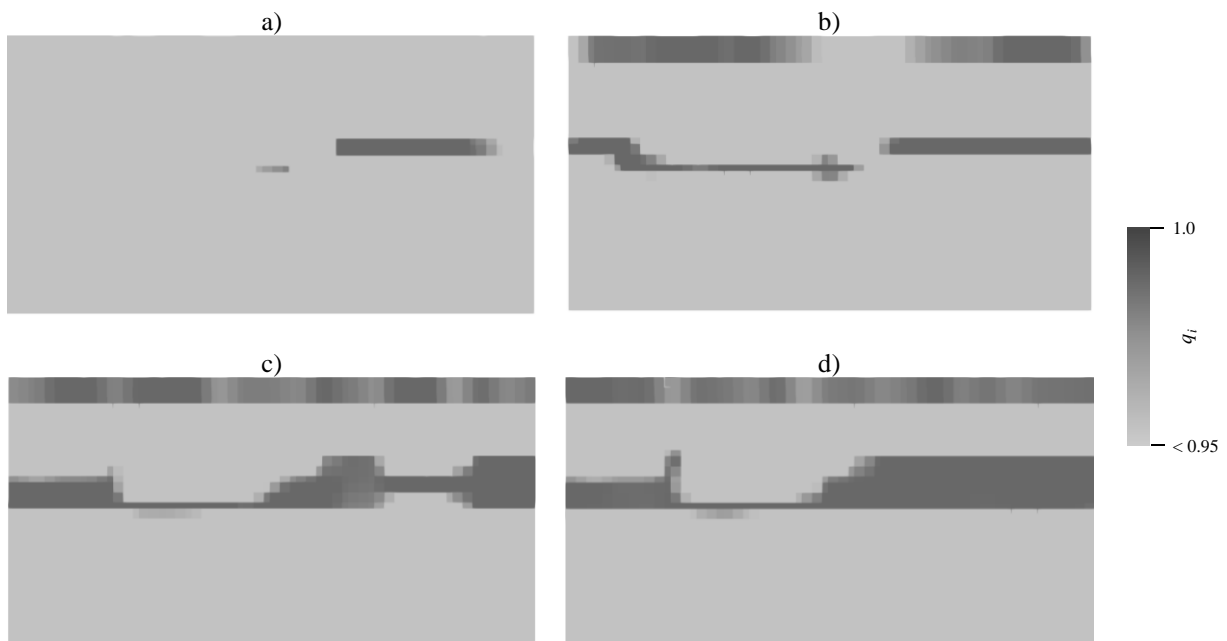

Figure 4. Typical 2D liquefaction evolution after a) 6 s, b) 7.2 s, c) 9 s, and d) 12 s.

Figure 5 shows a comparison between the end stage of the 2D domain and the combination of 1D columns (note that Figure 5a is the same as Figure 4d). In Figure 5b several characteristics of 1D simulations are observed. All the 1D columns have liquefied and exhibit typical horizontal liquefied layers. Compared to the 2D simulation, it is noticeable that the overall position of the liquefaction zones is consistent with the liquefaction occurring in the 2D domain. Nevertheless, due to the limitations of 1D simulations, liquefaction does not spread, and therefore A_L is significantly smaller compared to the 2D domain. Figure 6 shows an extension of the results of Figure 5. Figure 6a shows A_L with respect to time for each of the 1D columns of Figure 5b. Similarly to Figure 2b, all plots of 1D liquefaction exhibit step trends (i.e. instant vertical increments due to the liquefaction of full rows of Gauss points). Nevertheless, after combining the 1D results, a 1D mean response is obtained showing an apparently reasonable (but not necessarily reliable) solution. Figure 6b shows the comparison of A_L between the 2D domain, the mean value of the combined 1D columns and the 1D column of homogeneous material (i.e. $e_\mu = 0.75$). The results of the 1D columns, both the mean and the homogeneous cases, are similar. Both reach almost identical maximum values of $A_L = 7\%$. Nevertheless, the triggering times do not coincide, with the triggering time of the mean value being approximately one second earlier. On the other hand, the results of the 2D simulation are far-off from the 1D results. Although the triggering time may resemble the results from the 1D mean, the growth rate and the maximum value of A_L are different. As a result of 2D effects, liquefaction grows until reaching $A_L = 16.2\%$ (more than twice as much as the 1D results).
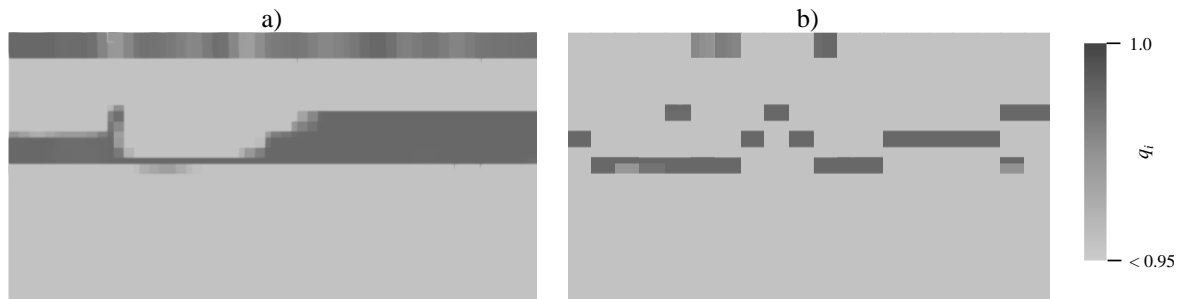

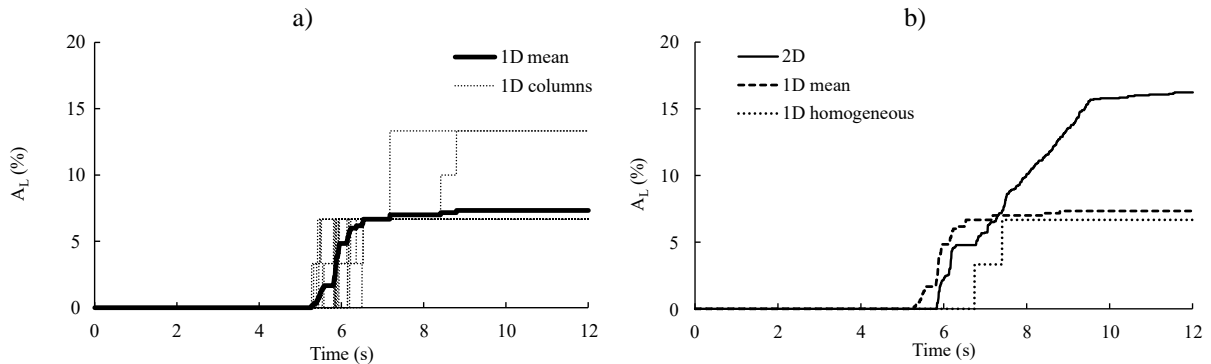**Figure 5**. Final liquefaction stage of the a) 2D domain, and b) the combined 1D columns.

Figure 6. Liquefaction area (A_L) of the a) 1D columns and the computed 1D mean , and b) the 2D domain, the computed 1D mean and the homogeneous 1D column using $e_\mu = 0.75$.

Figure 7 shows results for A_L from multiple realizations. Figure 7a shows the A_L of 2D domains (including the 2D plot of Figure 6b indicated as the original result). It is observed that A_L is reasonably consistent before 8 s. Most liquefaction events are triggered at around 6 s and values reach $A_L \approx 10 \%$ before 8 s. Nevertheless, results differ considerably afterwards. Some realizations reach $A_L \approx 8 \%$, which is equivalent to a thin layer of soil undergoing liquefaction (similar to 1D columns), whereas other analyses exhibit a wide range of results, reaching, in some cases, $A_L \approx 30 \%$. Similar to the computed 1D mean of Figure 6b, the 1D mean plots of the 2D realizations were computed and are shown in Figure 7b. In contrast to Figure 7a, it is observed that the variability of the results is much narrower. The triggering times and final values of A_L are similar and no liquefaction area growth is observed after the most intense interval of the earthquake occurred, indicating again the limitations of 1D simulations. Note that the use of the same set of statistics (i.e. e_μ, e_σ, θ_H and θ_V) produces a different distribution of void ratio's, hence returning different A_L between realizations.
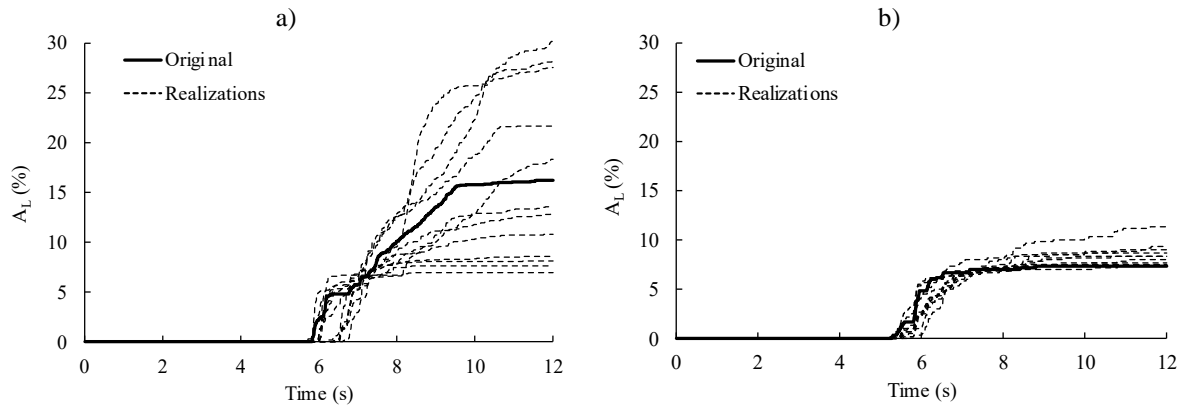
Figure 7. Liquefaction area (A_L) of a) 2D simulations, and b) their equivalent mean values using 1D columns.

Conclusions

Liquefaction has been studied through 1D and 2D simulations, considering homogeneous and heterogeneous soils and using a standard liquefaction index q_i. It has been shown that 1D simulations of homogeneous or heterogeneous materials exhibit uniform and horizontal liquefaction zones. The triggering of 1D simulations shows a stepped response, indicating instant liquefaction at the full width of the domain and, despite 1D columns of heterogeneous material being triggered at different times compared to the homogeneous simulation, the maximum liquefied area A_L reaches mostly similar values without indications of growing in time. In contrast to 1D simulations, 2D simulations show significant differences, of which the most important are the evolution of liquefaction in time and the significant increase in the total liquefied area. Due to the simplification of 1D simulations, differential horizontal and vertical movements are prevented. Therefore a continuous growth of the liquefaction area is not possible. 2D simulations demonstrate that liquefaction can grow even after the strongest amplitudes of an earthquake have occurred, due to the irregularity of the liquefied area that permits differential movement of the soil. Because of the continuous spread of liquefaction, extending until reaching a considerable area, significant settlements can occur afterwards.

Acknowledgments

References

Basu, D., Montgomery, J., and Stuedlein, A.W. (2019). Liquefaction-induced settlement estimates for a spatially variable deposit using numerical and empirical approaches. *Proceedings of the 7th International Symposium on Geotechnical Safety and Risk, Taipei*, 870-875.

Cook, R.D., Malkus, D.S., and Plesha, M.E. (1989). *Concepts and Applications of Finite Element Analysis*. Third edn. John Wiley & Sons Ltd.

Fenton, G.A., and VanMarcke, E.H. (1998). Spatial variation in liquefaction risk. *Géotechnique,* 48(6), 819-831.

Griffiths, D.V., and Fenton, G.A. (2004). Probabilistic slope stability analysis by finite elements. *Journal of Geotechnical and Geoenvironmental Engineering*, 130(5), 507-518.

Gudehus, G., Amorosi, A., Gens, A., Herle, I., Kolymbas, D., Mašín, D., Wood, D.M., Niemunis, A., Nova, R., Pastor, M., Tamagnini, A., and Viggiani, G. (2008). The soilmodels. info project. *International Journal for Numerical and Analytical Methods in Geomechanics*, 32(12), 1571-1572.

Hicks, M.A., Onisiphorou, C. (2005). Stochastic evaluation of static liquefaction in a predominantly dilative sand fill. *Géotechnique,* 55(2), 123-133.

Niemunis, A., and Herle, I. (1997). Hypoplastic model for cohesionless soils with elastic strain range. *Mechanics of Cohesive-frictional Materials,* 2(4), 279-299.

Popescu, R., Prevost, J.H., and Deodatis, G. (2005). 3D effects in seismic liquefaction of stochastically variable soil deposits. *Géotechnique,* 55(1), 21-31.

Seed, H.B. (1979). Soil liquefaction and cyclic mobility evaluation for level ground during earthquakes. *Journal of the Geotechnical Engineering Division*, 105(2), 201-255.

van den Eijnden, A.P., and Hicks, M.A. (2017). Efficient subset simulation for evaluating the modes of improbable slope failure. *Computers and Geotechnics*, 88, 267-280.

Varkey, D., Hicks, M.A., van den Eijnden, A.P., Vardon, P.J. (2020). On characteristic values for calculating factors of safety for dyke stability. *Géotechnique Letters,* 10(2), 353-359.

Zienkiewicz, O.C., Chan, A.H.C., Pastor, M., Schrefler, B.A., and Shiomi, T. (1999). *Computational Geomechanics with Special Reference to Earthquake Engineering.* John Wiley & Sons Ltd.